ORIGINAL ARTICLE

Neuropathology and Applied Neurobiology

JOURNAL OF THE BRITISH NEUROPATHOLOGICAL SOCIETY

WILEY

Pathogenic *DPAGT1* variants in limb-girdle congenital myasthenic syndrome (LG-CMS) associated with tubular aggregates and ORAI1 hypoglycosylation

Laura vanden Brande[1,2] | Stéphanie Bauché[1,3] | Laura Pérez-Guàrdia[4] |
Damien Sternberg[5] | Andreea M. Seferian[2] | Edoardo Malfatti[1,6] |
Roberto Silva-Rojas[4] | Clémence Labasse[1] | Frédéric Chevessier[1] |
Pierre Carlier[1] | Bruno Eymard[1,6] | Norma B. Romero[1] | Jocelyn Laporte[4] |
Laurent Servais[7,8] | Teresa Gidaro[1,2] | Johann Böhm[4]

[1]Institut de Myologie, GHU La Pitié-Salpêtrière, Paris, France

[2]Sorbonne Université, Institut I-MOTION, Hôpital Armand Trousseau, Paris, France

[3]Inserm U 1127, CNRS UMR 7225, Sorbonne Universités, UPMC Université Paris 06 UMR S 1127, Institut du Cerveau et de la Moelle épinière, ICM, Paris, France

[4]Departement of Translational Medicine and Neurogenetics, IGBMC (Institut de Génétique et de Biologie Moléculaire et Cellulaire), Inserm U1258, CNRS UMR7104, Université de Strasbourg, Illkirch, France

[5]Service de Biochimie Métabolique, UF Cardiogenetics and Myogenetics, Hôpital de la Pitié-Salpêtrière, APHP, Paris, France

[6]Centre de Référence de Pathologie Neuromusculaire Paris-Est, Groupe Hospitalier Pitié-Salpêtrière, Paris, France

[7]MDUK Oxford Neuromuscular Centre and NIHR Oxford Biomedical Research Centre, University of Oxford, Oxford, UK

[8]Neuromuscular Reference Center, Department of Paediatrics, University Hospital of Liège, Liège, Belgium

Correspondence
Johann Böhm, IGBMC, 1 Rue Laurent Fries, Illkirch 67404, France.
Email: johann@igbmc.fr

Abstract

Aims: Limb-girdle congenital myasthenic syndrome (LG-CMS) is a genetically heterogeneous disorder characterised by muscle weakness and fatigability. The LG-CMS gene *DPAGT1* codes for an essential enzyme of the glycosylation pathway, a posttranslational modification mechanism shaping the structure and function of proteins. In *DPAGT1*-related LG-CMS, decreased glycosylation of the acetylcholine receptor (AChR) reduces its localization at the neuromuscular junction (NMJ) and results in diminished neuromuscular transmission. LG-CMS patients also show tubular aggregates on muscle biopsy, but the origin and potential contribution of the aggregates to disease development are not understood. Here, we describe two LG-CMS patients with the aim of providing a molecular diagnosis and to shed light on the pathways implicated in tubular aggregate formation.

Methods: Following clinical examination of the patients, we performed next-generation sequencing (NGS) to identify the genetic causes, analysed the biopsies at the histological and ultrastructural levels, investigated the composition of the tubular aggregates and performed experiments on protein glycosylation.

Results: We identified novel pathogenic *DPAGT1* variants in both patients and pyridostigmine treatment quantitatively improved muscle force and function. The tubular

aggregates contained proteins of the sarcoplasmic reticulum (SR) and structurally conformed to the aggregates observed in tubular aggregate myopathy (TAM). TAM arises from overactivation of the plasma membrane calcium channel ORAI1, and functional studies on muscle extracts from our LG-CMS patients evidenced abnormal ORAI1 glycosylation.

Conclusions: We expand the genetic variant spectrum of LG-CMS and provide a genotype/phenotype correlation for pathogenic *DPAGT1* variants. The discovery of ORAI1 hypoglycosylation in our patients highlights a physiopathological link between LG-CMS and TAM.

K E Y W O R D S
DPAGT1, glycosylation, LG-CMS, limb-girdle congenital myasthenic syndrome, ORAI1, tubular aggregates

INTRODUCTION

Congenital myasthenic syndromes (CMS) are a clinically and genetically heterogeneous group of disorders characterised by fluctuating muscle weakness and fatigability. They are caused by impaired signal transmission at the neuromuscular junction (NMJ), constituting the relay between motor neuron and muscle fibre and taking a central role in the conversion of an electrical stimulus into muscle contraction. To date, more than 30 CMS genes have been identified, and they essentially code for presynaptic, synaptic or postsynaptic proteins or proteins involved in the maturation or maintenance of the NMJ [1, 2].

Limb-girdle congenital myasthenic syndrome (LG-CMS) is a subtype of CMS, and affected individuals typically present with predominant proximal weakness, while ocular, bulbar and facial muscles are spared or only minimally affected [3, 4]. LG-CMS is caused by pathogenic variants in *AGRN*, *ALG2*, *ALG14*, *COLQ*, *DOK7*, *DPAGT1*, *GFPT1*, *GMPPB*, *LRP4* or *MUSK*, either encoding proteins implicated in NMJ signalling or the glycosylation pathway [5–14]. Glycosylation is a major posttranslational modification mechanism and substantially modulates the structure and function of a wide variety of proteins including the acetylcholine receptor (AChR) or the Ca^{2+} regulators STIM1 (Stromal Interaction Molecule 1) and ORAI1 (named after the Horai, the goddesses of the seasons in Greek mythology). AChR assembly and export to the cell surface of the postsynaptic NMJ compartment require glycosylation, and deficient AChR glycosylation results in reduced synaptic response to acetylcholine, representing the main pathomechanism underlying the transmission defects in LG-CMS [5, 6, 15, 16]. The Ca^{2+} sensor STIM1 and the Ca^{2+} channel ORAI1 control cellular Ca^{2+} homeostasis through the ubiquitous store-operated Ca^{2+} entry (SOCE) mechanism, and incomplete STIM1 and ORAI1 glycosylation were shown to interfere with normal SOCE function [17, 18]. However, the relevance of STIM1 and ORAI1 glycosylation in the development of LG-CMS has not been investigated.

To date, nine LG-CMS families with pathogenic *DPAGT1* variants have been reported [6, 19–23], allowing only a narrow view of the clinical and genetic spectrum of the disorder and precluding a full understanding of the underlying pathomechanisms. Here, we describe

Key Points

- Limb-girdle congenital myasthenic syndrome (LG-CMS) is clinically characterised by muscle weakness and fatigability. One of the causative genes is *DPAGT1*, encoding an essential enzyme of protein glycosylation.
- LG-CMS patients exhibit tubular aggregates on muscle biopsies, but the origin and contribution of these aggregates to disease development are not understood.
- We describe two novel *DPAGT1* patients and provide clinical, genetic, histological, ultrastructural and functional data.
- Analysis of the aggregates uncovered their composition and showed that they are comparable to the aggregates characterising tubular aggregate myopathy (TAM). TAM is caused by pathogenic variants in the calcium channel ORAI1.
- Functional investigations evidenced ORAI1 hypoglycosylation in our patients, providing a physiopathological link between LG-CMS and TAM.

two unrelated LG-CMS patients with novel pathogenic *DPAGT1* variants. Both presented with childhood-onset limb-girdle muscle weakness, abnormal electroneuromyogram (ENMG) findings with decremental response to repetitive nerve stimulation and tubular aggregates on the muscle biopsies. Tubular aggregates can be seen in various muscle disorders and constitute the histopathological hallmark of tubular aggregate myopathy (TAM). TAM is caused by pathogenic variants in the Ca^{2+} buffer calsequestrin (CASQ1) [24, 25], the Ca^{2+} sensor STIM1 [26] or the Ca^{2+} channel ORAI1 [27], and involves skeletal muscle, bone, spleen, skin and platelet anomalies [28, 29]. We illustrate that the tubular aggregates in our patients contain STIM1, calsequestrin, RyR1, SERCA and the LG-CMS protein GFPT1, and we show that ORAI1 is abnormally glycosylated, establishing a

PATHOGENIC *DPAGT1* VARIANTS IN LIMB-GIRDLE CONGENITAL MYASTHENIC SYNDROME (LG-CMS) ASSOCIATED WITH TUBULAR AGGREGATES AND ORAI1 HYPOGLYCOSYLATION

Neuropathology and Applied Neurobiology

JOURNAL OF THE BRITISH NEUROPATHOLOGICAL SOCIETY

WILEY

3 of 13

physiopathological link between LG-CMS and TAM and providing insight into the formation of tubular aggregates in myasthenia.

MATERIALS AND METHODS

Patients

DNA samples and photographs were taken for diagnostic purposes and with written informed consent from the patients or legal guardians according to the declaration of Helsinki and its later amendments. DNA storage and utilisation followed institutional IRB-accepted protocols (DC-2012-1693). Patients were from metropolitan France (Family 1) and the French overseas department Guadeloupe (Family 2).

The handgrip and pinch strength and function were measured using MyoGrip, MyoPinch and Moviplate following a previously described protocol [30] and compared to predictive age-matched control values [31].

Sequencing and segregation analysis

Patient 1 was sequenced for a targeted panel of 54 genes implicated in muscle excitation including 30 CMS genes using a SeqCapEZ capture design (NimbleGen, Madison, United States) and a MiSeq sequencer (Illumina, San Diego, United States). For Patient 2, exome sequencing was carried out using the SureSelect Human All Exon Kit v5 (Agilent, Santa Clara, United States) and the Illumina HiSeq 2500 system. Sequence data were aligned to the GRCh37/hg19 reference genome, and variants were filtered based on their frequency in gnomAD (http://gnomad.broadinstitute.org/) and our in-house database containing >1,500 exomes, segregation, expression pattern and the known implication of the respective genes in human disorders. Pathogenic impacts were predicted using the Genodiag bioinformatics pipeline or Alamut v.2.5 (http://www.interactive-biosoftware.com). Sanger sequencing was applied for segregation analyses in both families. The variants were numbered according to GenBank NM_001382.3 and NP_001373.2.

Histology and electron microscopy

Both patients underwent open muscle biopsies for morphological analyses. For histology and histochemistry, transverse sections (10 μm) were stained with haematoxylin and eosin (H&E), Gömöri trichrome, NADH tetrazolium reductase (NADH-TR), succinate dehydrogenase (SDH) and ATPase, and digital photographs were obtained with the AxioCam HRc camera (Zeiss, Oberkochen, Germany). For electron microscopy, the muscle samples were fixed with glutaraldehyde (2.5%, pH 7.4), post-fixed with osmium tetroxide (2%), incubated with 5% uranyl acetate, dehydrated in graded series of ethanol and embedded in epon resin 812. Grids were viewed on Met Jeol 1400 Flash electron microscope (Jeol, Tokyo, Japan).

Expression studies

For quantitative PCR (RT-qPCR), RNA was extracted from the muscle specimen from Patient 1 and reverse transcribed with the SuperScript™ IV (ThermoFisher Scientific, Waltham, United States). The cDNA was amplified using the SYBR Green Master Mix I on a LightCycler 480 Real-Time PCR System (both Roche Diagnostics, Basel, Switzerland). Forward and reverse primers are listed below. Primer specificity was determined through melting curve analyses and Sanger sequencing of the PCR products. *RPL27* served as a reference gene [32].

Gene	Forward	Reverse
RPL27	5′-GGG TGG TTG CTG CCG AA-3′	5′-GCC ATC ATC AAT GTT CTT CAC GA-3′
GFPT1	5′-GCA ATC TCT CTC GTG TGG AC-3′	5′-CCA CTA CTG CTG CAA CAT CA-3′
DPAGT1	5′-ACC TAC AGC TGC CTC ACT AC-3′	5′-ATG ACT AGT GAC TGG CCA GC-3′
OST4	5′-AAG CAG GAA TGA AAG TGG CG-3′	5′-GTG GCA GCT TCT TGT TCC AT-3′

Protein studies

For glycosylation studies, muscle samples were homogenised in RIPA (radio immunoprecipitation) buffer supplemented with 1mM PMSF and a complete EDTA-free protease inhibitor cocktail (Roche). To remove the N-linked oligosaccharides from ORAI1, samples were incubated in glycoprotein denaturing buffer at 100°C for 10 min to inactivate the protease inhibitors and then supplemented with Glyco-Buffer, NP-40 and 1 μl of PNGase F (P0704S, New England BioLabs, Ipswich, United States) and incubated at 37°C for 60 min.

Denatured proteins were loaded on an 8% SDS-PAGE gel, which was transferred to a nitrocellulose membrane using the Transblot Turbo TM RTA Transfer Kit (Biorad, Hercules, United States). The following primary and secondary antibodies were used: mouse anti-ORAI1 (sc-377281, Santa Cruz Biotechnology, Dallas, United States) and peroxidase-coupled goat anti-mouse (115-036-068, Jackson ImmunoResearch, Ely, United Kingdom). Finally, samples were analysed on the Amersham Imager 600 (GE Healthcare Life Sciences, Chicago, IL, United States). Ponceau S staining was used as a protein loading control.

For immunofluorescence, 10 μm sections were fixed and incubated with the following antibodies: rabbit anti-STIM1 (AB9870, Millipore, Burlington, United States), mouse anti-calsequestrin (Affinity BioReagents, Golden, United States), mouse anti-Ryanodine receptor Clone 34C (R-12, Sigma-Aldrich, Saint Louis, United States), mouse anti-SERCA1 (IIH11, Novocastra, Newcastle, United Kingdom), mouse anti-SERCA2 (IID8, Novocastra), mouse anti-GFPT1 (bs13341R, Bioss Antibodies, Woburn, United States), rabbit anti-DPAGT1 (MA5-31738, ThermoFisher Scientific) and appropriate Alexa Fluor secondary antibodies (Invitrogen, Carlsbad, United States).

TABLE 1   Clinical and histological features of LG-CMS patients with DPAGT1 mutations.

	Family 1	Family 2	Family 3	Family 4	Family 5
Reference	Selcen et al. [22]	Klein et al. [20]	Bogdanova et al. [19]	This report	Belaya et al. [6]; Finlayson et al. [23]
DPAGT1 variant(s)	c.1A>C (p.Met1Leu) c.1123C>T (p.His375Tyr)	c.85A>T (p.Ile29Phe) c.88C>T (p.Pro30Ser)	c.135_136delCC (p.Leu46fs*) c.367C>T (p.Arg123Cys)	c.271C>T (p.Pro91Ser) c.380_395dup (p.Ser133fs*64)	c.324G>C (p.Met108Ile) c.349G>A (p.Val117Ile)
Affected individuals	2	1	2	1	1
Disease onset	Infancy	Infancy	Infancy	Childhood	Childhood
Age at last clinical examination	13/12	14	Adulthood	49	43
Predominant muscle involvement	Proximal limb, hand, facial, axial weakness	Shoulder girdle, distal hand & finger extensor weakness	Upper limbs and finger extensor weakness	Limb-girdle weakness	Limb-girdle, neck, finger abductor & extensor, ankle dorsiflexion weakness
Eye movement defects	No	Restricted abduction	No	No	No
Respiration	Normal	Normal	Normal	VC 76%	VC 70%
Gait abnormalities	Wheelchair since age 5/ambulant at age 12	Yes	Waddling gait	Restricted walking perimeter	Wheelchair since age 9
Contractures	No	Fingers	No	Ankles	Fingers, elbows, knees, ankles
EMG	CMAP decrement 16–41%	Increased jitter	Myopathic	CMAP decrement	Increased jitter
Muscle histology	Type I fibre atrophy, tubular aggregates, autophagic vacuoles	Type I fibre atrophy, fibre size variability	Fibre atrophy, fibre size variability	Fibre size variability, type I fibre predominance, tubular aggregates	Tubular aggregates
Muscle ultrastructure	Abnormal NMJ, mitochondrial degeneration, myofibre disorganisation, autophagic vacuoles	NA	NA	Abnormal NMJ, mitochondrial degeneration	NA
Other features	Learning disabilities, scoliosis, reduced tendon reflexes, long QTc interval at ECG, autistic spectrum disorder	Learning disabilities, scoliosis, joint hyperlaxity	Learning disabilities, facial dysmorphism	Joint hyperlaxity, paraesthesia	-

Note: Homozygous mutations are in bold, and novel cases are highlighted in grey.
Abbreviations: NA, not assessed; VC, vital capacity.

PATHOGENIC *DPAGT1* VARIANTS IN LIMB-GIRDLE CONGENITAL MYASTHENIC SYNDROME (LG-CMS) ASSOCIATED WITH TUBULAR AGGREGATES AND ORAI1 HYPOGLYCOSYLATION

Neuropathology and Applied Neurobiology
JOURNAL OF THE BRITISH NEUROPATHOLOGICAL SOCIETY
WILEY | 5 of 13

TABLE 1 (Continued)

	Family 6	Family 7	Family 8	Family 9	Family 10	Family 11
Reference	Belaya et al. [6]; Finlayson et al. [23]	Belaya et al. [6]; Finlayson et al.	Selcen et al. [22]	Belaya et al. [6]; Finlayson et al. [23]	Basiri et al. [21]	This report
DPAGT1 variant(s)	c.349G>A (p.Val117Ile); c.699dupC (p.Thr234fs*116)	c.358C>A (p.Leu120Met); c.791 T>G (p.Val264Gly)	c.360G>C (p.Leu120Leu); c.790G>A (p.Val264Met)	c.478G>A (p.Gly160Ser); c.574G>A (p.Gly192Ser)	**c.652C>T (p.Arg218Trp)**	**c.1133A>T (p.Asn378Ile)**
Affected individuals	1	2	1	1	4	1
Disease onset	Childhood	Infancy	Childhood	Childhood	Childhood/adolescence	Infancy
Age at last clinical examination	53	17	14	48	34	13
Predominant muscle involvement	Limb-girdle, neck weakness	Limb-girdle, neck weakness	Proximal limb and finger extensor weakness	Limb-girdle, neck, finger abductor & extensor, ankle dorsiflexion weakness	Proximal lower limb weakness, cramps, amyotrophy	Shoulder girdle, finger extensors, and tibialis anterior weakness
Eye movement defects	No	No	Lateral gaze restrictions	No	No	No
Respiration	VC 64%	Normal	Normal	Normal	Ventilation since age 15	Ventilation since age 8
Gait abnormalities	Waddling gait	No	Intoeing footdrop	Wheelchair since age 14	Yes	Steppage gait
Contractures	No	No	No	No	No	Hips, ankles
EMG	Increased jitter	Increased jitter	CMAP decrement 20%	Increased jitter	CMAP decrement 40%, fibrillations	CMAP decrement
Muscle histology	Tubular aggregates, abnormal NMJ	Tubular aggregates	Type I fibre atrophy, tubular aggregates, autophagic vacuoles	Tubular aggregates, vacuoles, glycogen accumulations	Fibre size variability, atrophy, fatty replacements, internalised nuclei	Fibre size variability, tubular aggregates
Muscle ultrastructure	NA	NA	Abnormal NMJ, mitochondrial degeneration, myofibre disorganisation, autophagic vacuoles	NA	NA	Abnormal NMJ
Other features	Scoliosis, abnormal ECG	Learning disabilities, scoliosis	Learning disabilities, cubitus valgus	Learning disabilities, scoliosis, pes cavus, abnormal ECG	Reduced tendon reflexes, dysarthria, scoliosis	Learning disabilities, dysarthria

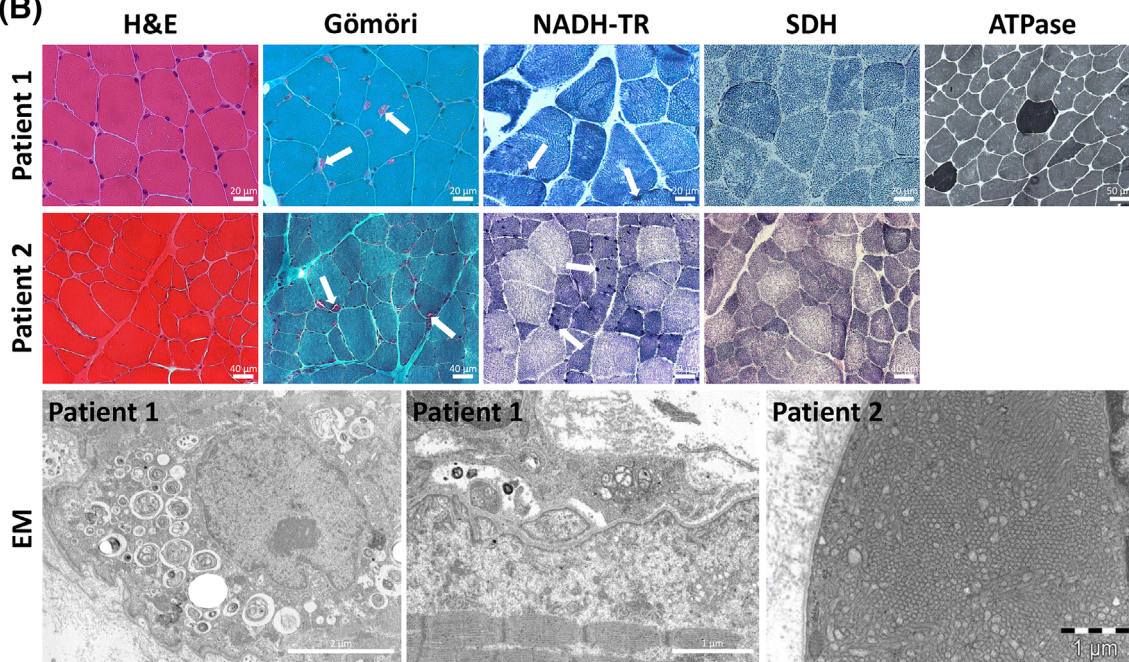*Note:* Homozygous mutations are in bold, and novel cases are highlighted in grey.
Abbreviations: NA, not assessed; VC, vital capacity.
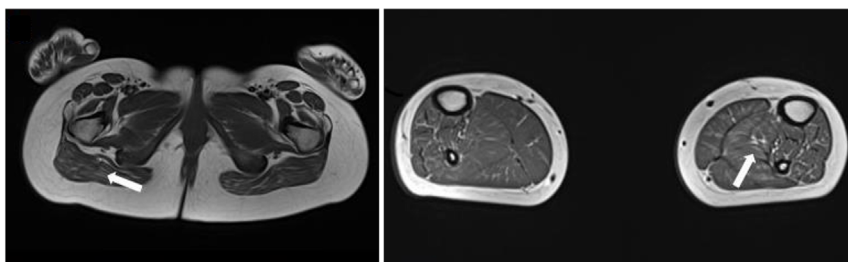
FIGURE 1   MRI, muscle histology and ultrastructure of *DPAGT1* patients. (A) MRI of Patient 2 revealed general hypotrophy and fatty infiltration in the pelvic girdle and lower leg muscles with particular involvement of the gluteus maximus and soleus (arrows). (B) Histological and histochemical analysis of muscle sections from both patients uncovered fibre size variability, accumulations appearing in red on Gömöri stain and blue on NADH-TR (arrows) and predominance of light type I myofibres on ATPase stain (pH 9.4). Electron microscopy detected numerous vacuoles (left), a strong reduction of postsynaptic folds and poorly developed nerve endings at the neuromuscular junction (middle), as well as densely packed tubular aggregates (right) in both patients.

Sections were mounted with an antifade reagent (Invitrogen), and images were acquired on a Zeiss AxioPhot fluorescence microscope (Zeiss Oberkochen, Germany).
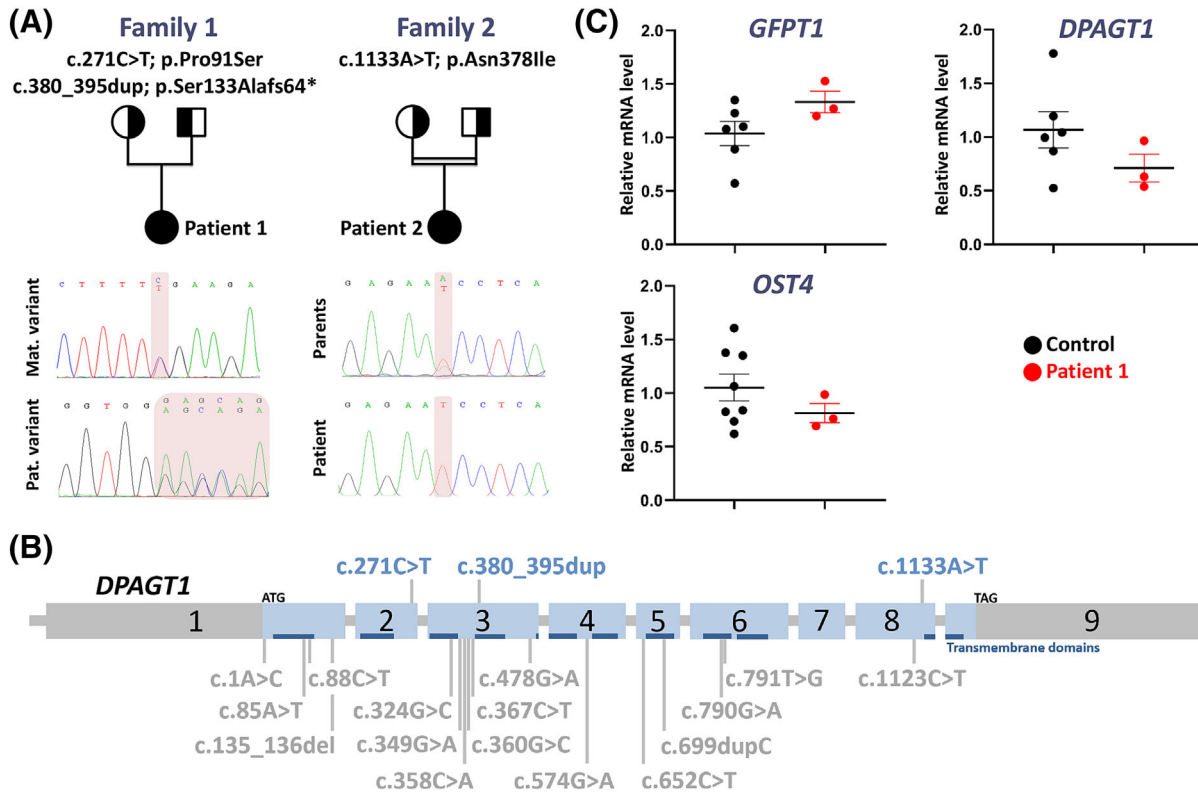
RESULTS

The patients described here belong to two unrelated families. The clinical and histopathological features are summarised in Table 1 and compared with all previously reported LG-CMS patients harbouring pathogenic *DPAGT1* variants.

Clinical description

Patient 1 presented with childhood-onset fluctuating upper and lower limb muscle weakness, gait abnormalities and frequent falls.

The patient was never able to run, and motor performance worsened with increasing temperature. At the age of 39, the patient experienced marked generalised muscle weakness for 6 months and fluctuating fatigability, and clinical examination revealed limb-girdle muscle weakness as well as amyotrophy of the scapular and forearm muscles. Bulbar or oculomotor defects were not noted. The fluctuation was striking with a decrease in arm abduction from 60° to 20° and in hip flexion, in the lying position, from 75 s to 5 s within the same day. The patient also manifested mild Achilles tendon retractions and a reduced vital capacity (VC) of 76%, while CK levels were within normal limits (134 U/L). ENMG revealed normal motor nerve conduction, but repetitive nerve stimulation disclosed a 20% decrease in compound muscle action potential (CMAP) in both upper and lower limbs. At the last clinical examination at the age of 49, the patient had fluctuating and slightly deteriorating muscle weakness, difficulties getting up from a chair and a decrease of walking distance limited to 1 km.

PATHOGENIC *DPAGT1* VARIANTS IN LIMB-GIRDLE CONGENITAL MYASTHENIC SYNDROME (LG-CMS) ASSOCIATED WITH TUBULAR AGGREGATES AND ORAI1 HYPOGLYCOSYLATION

Neuropathology and Applied Neurobiology
JOURNAL OF THE BRITISH NEUROPATHOLOGICAL SOCIETY
WILEY

7 of 13

FIGURE 2 Pathogenic *DPAGT1* variants and impact on gene expression. (A) Pedigrees and electropherograms showing the segregation of the *DPAGT1* variants in both families. Patient 1 is compound heterozygous with one variant on the maternal allele and one variant on the paternal allele, while Patient 2 carries a homozygous variant with both parents in the heterozygous state. (B) Schematic representation of the *DPAGT1* exons and position of the known (grey) and novel (blue) LG-CMS variants. Dark stripes indicate the segments encoding the transmembrane domains. (C) RT-qPCR on muscle extracts from Patient 1 and an age-matched control revealed comparable expression levels of the glycosylation genes *GFPT1*, *DPAGT1* and *OST4*.

Patient 2 was born to healthy consanguineous parents. Pregnancy and birth were unremarkable. Hypotonia and fatigability involving frequent falls were noticed at 18 months. The patient was unable to run or climb stairs and manifested speech delay, dysarthria requiring speech therapy, and learning disabilities. In this context, brain MRI was performed at 6 years of age but did not reveal any abnormalities. Polysomnography at 8 years disclosed obstructive sleep apnoea hypopnoea syndrome (OSAHS), and non-invasive nocturnal ventilation was initiated. At age 13, the patient had a positive Gower's sign, steppage gait and axial, proximal and distal muscle weakness predominantly affecting the shoulder girdle, finger extensors and the tibialis anterior. Contractures of the ankles and hips were also noted, abduction of the arms was limited to 45° and CK was normal or mildly elevated (223 U/L). Repetitive stimulation of the axillary nerve at the trapezius muscle disclosed a CMAP decrement of 50.8%. Muscle MRI demonstrated global hypotrophy of axial and appendicular musculature, with fatty infiltration of the gluteal area and the lower limb with particular involvement of the gluteus maximus and the soleus (Figure 1A).

Tubular aggregates and structural NMJ defects on muscle biopsies

To correlate the muscle weakness with myofiber morphology, we examined quadriceps biopsies from both patients. Histological and histochemical analyses of the muscle sections revealed fibre size variability on H&E stain, marked type I fibre predominance on ATPase, as well as perinuclear and subsarcolemmal aggregates appearing in bright red on Gömöri trichrome (Figure 1B). The aggregates also stained dark blue on NADH-TR, were undetectable on SDH and were identified as densely packed membrane tubules by electron microscopy (Figure 1B). We also observed vacuoles and ultrastructural alterations of the NMJ architecture with major remodelling of the endplates, loss of junctional folds and poorly developed nerve endings. Taken together, the clinical presentation of the patients, the ENMG findings and the architectural myofiber and NMJ anomalies were strongly indicative of LG-CMS.

Identification of novel pathogenic *DPAGT1* variants and impact on gene expression

To investigate the genetic causes of the LG-CMS phenotype in our patients, we performed panel or exome sequencing, and we identified causative *DPAGT1* variants in both families (Figure 2A). Patient 1 carries a heterozygous c.271C>T (p.Pro91Ser) missense variant in exon 2 on the maternal allele and a heterozygous c.380_395dup duplication of 16 nucleotides in exon 3 on the paternal allele, confirming recessive disease inheritance. The TGCTACCTACAGCTGC duplication is predicted to lead to a shift of the reading frame and the occurrence of a premature stop codon (p.Ser133Alafs64*) and

presumably involves nonsense-mediated mRNA decay. Patient 2 harbours a homozygous c.1133A>T (p.Asn378Ile) missense variant in *DPAGT1* exon 8, and both parents were found to be heterozygous.

DPAGT1 codes for UDP-N-acetylglucosamine-dolichyl-phosphate N-acetylglucosaminephosphotransferase, an enzyme catalysing an early step of the N-glycosylation pathway. It resides in the ER membrane and contains 10 transmembrane domains. The c.271C>T (p.Pro91Ser) missense variant affects an amino acid in the luminal loop connecting transmembrane domains 2 and 3, and the c.1133A>T (p.Asn378Ile) missense variant affects an amino acid in the cytosolic loop before transmembrane domain 10 (Figure 2B). The novel and previously reported *DPAGT1* variants are distributed over the entire gene
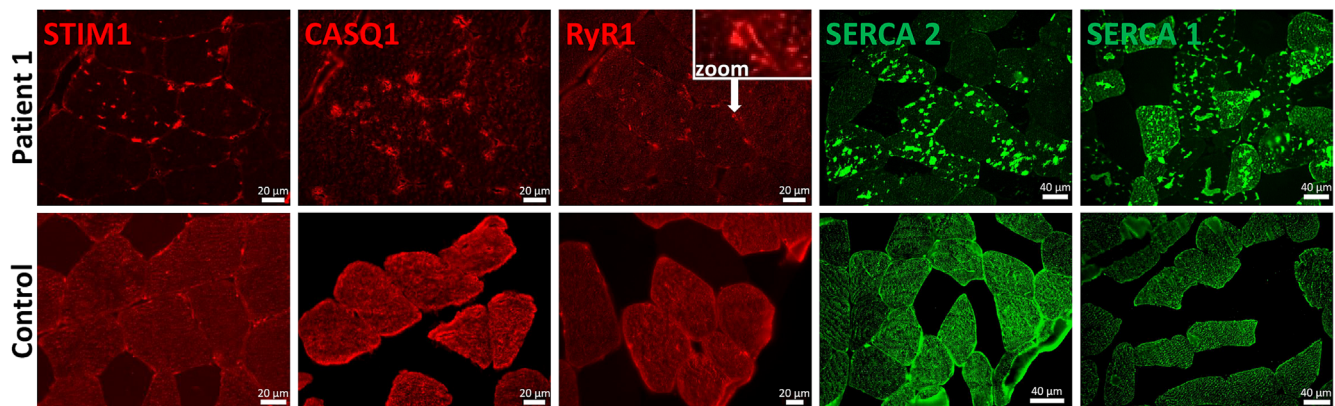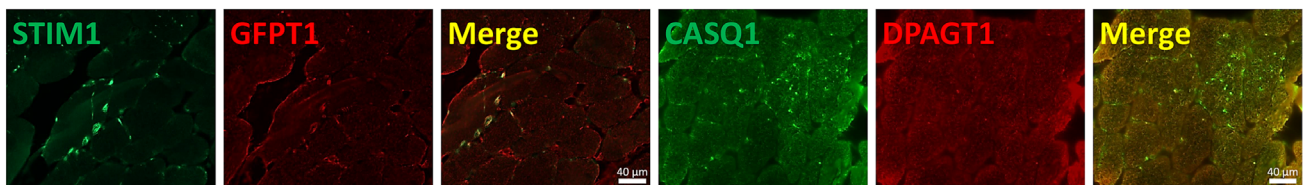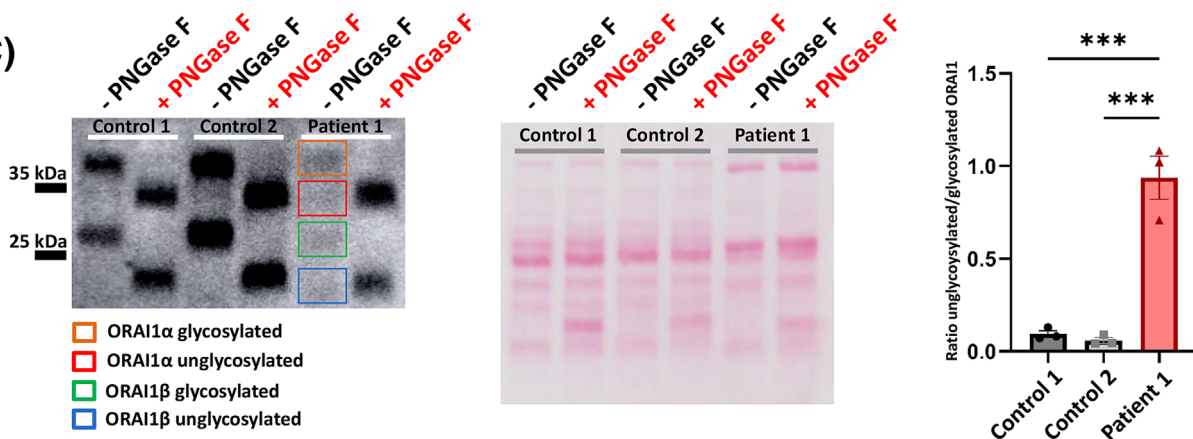

FIGURE 3 Tubular aggregate composition and functional impact of the *DPAGT1* variants. (A) In Patient 1, the tubular aggregates contained STIM1, calsequestrin (CASQ1), RyR1, SERCA1 and SERCA2. Note the peripheral RyR1 localization within the aggregates (arrow and zoom). Muscle sections from a healthy individual served as control. (B) GFPT1 but not DPAGT1 was found in the tubular aggregates in Patient 1. (C) The ORAI1 isoforms ORAI1α (upper band) and ORAI1β (lower band) are glycosylated in the control muscle samples, and PNGase F treatment led to the cleavage of the oligosaccharides and the migration of both ORAI1 isoforms at a lower molecular weight. In untreated *DPAGT1* muscle samples from Patient 1, glycosylated and unglycosylated ORAI1α and ORAI1β coexist. The graph illustrates the ratio of unglycosylated versus glycosylated ORAI1 in control and patient muscle samples. It shows the mean ± SEM and significant differences are indicated as ***$P < 0.001$.

and do not point to a specific mutation hotspot. However, several pathogenic variants were detected in the segment coding for the cytoplasmic loop between the 3rd and 4th transmembrane domain, indicating that the affected protein domain plays an important role in the development of LG-CMS.

To investigate a potential impact of the identified *DPAGT1* variants on gene expression, we performed RT-qPCR on muscle extracts from Patient 1 and an age-matched control. We detected a moderate but non-significant reduction of *DPAGT1* expression, probably reflecting partial mRNA degradation resulting from the frameshift variant (Figure 2C). The mRNA levels of Glucosamine-fructose-6-phosphate aminotransferase isomerizing 1 (*GFPT1*) and oligosaccharyltransferase (*OST4*), respectively, acting upstream and downstream of DPAGT1 were comparable in Patient 1 and the control sample. This suggests that the *DPAGT1* variants do not substantially interfere with the transcriptional regulation of the N-glycosylation pathway.

Both c.271C>T (p.Pro91Ser) and c.1133A>T (p.Asn378Ile) missense variants have never been reported before, while the duplication of 16 nucleotides (c.380_395dup) is listed three times in the heterozygous state in gnomAD (http://gnomad.broadinstitute.org/), comprising more than 250,000 control alleles. In general, *DPAGT1* nonsense or frameshift variants are rare and never listed in the homozygous state in the public SNP databases, suggesting that the total loss of the protein is incompatible with life. This is also supported by the observation that all previously reported LG-CMS patients either carry two *DPAGT1* missense variants or a combination of a missense and a frameshift variant (Table 1).

There is no obvious genotype/phenotype correlation with regard to the type and position of the pathogenic *DPAGT1* variants in the novel and previously reported LG-CMS families. The first signs of a muscle disorder occurred in infancy or childhood, and all patients presented with a progressive but not life-threatening disease course. Some were wheelchair-bound since childhood or adolescence (Families 1, 5 and 9), while others were still ambulant with minor gait abnormalities in adulthood (Families 3, 4, 6 and 10). Muscle weakness essentially affected the limb girdles (7×), limbs and hands (7×) and neck (4×), and additional clinical features included learning disabilities (7×); scoliosis (6×); contractures of fingers, elbows, hips, knees or ankles (4×); abnormal respiration partially requiring ventilation (4×); cardiac anomalies (3×); joint hyperlaxity (2×); reduced tendon reflexes (2×); dysarthria (2×); and eye movement defects (2×). In a previously described family with two affected siblings, one was ambulant at the age of 12, while the other was more severely affected and wheelchair-bound since the age of 5 years [22], demonstrating intrafamilial variability and supporting the absence of a strict correlation between distinct *DPAGT1* variants and the clinical LG-CMS picture.

Positive response to pyridostigmine treatment

Based on the encouraging reports of *DPAGT1* patients treated with acetylcholine esterase inhibitors [6, 20], Patient 2 underwent a gradually increased therapy of up to 7.7 mg/kg pyridostigmine per day.

After 21 days of treatment, the patient performed slightly better on the 6-min walk test (6MWT) with 506 m compared to 490 m before treatment, but without reaching a clinically significant improvement of 30 m [33]. We also evaluated muscle strength and functional assessment using the Myogrip, MyoPinch and Moviplate devices [30]. While the maximal grip strength expressed in normal and age-related values remained unchanged, the pinching force of the index finger and thumbs improved by 28% (2.38 vs 1.5 kg) in the left hand and by 21% in the right hand (2.04 vs 1.69 kg). We also observed a significant improvement of the Moviplate score (+14%, reflecting the ability to repeat a flexion/extension movement of the wrist over 30 s) in the left hand, while the values in the right hand were comparable before and after treatment. Repetitive stimulation of the axillary nerve evidenced a decrement of 50.8% before treatment and 36% after pyridostigmine administration. Pyridostigmine treatment was pursued with regular assessment of muscle force and an adjustment of up to 8.5 mg/kg per day. After 6 months of treatment, the individual performances of the patient remained largely constant with 475 m on the 6MWT, a pinching force of 2.3 kg (left) and 2.1 kg (right) and stable Moviplate scores.

Treatment of Patient 1 with the acetylcholinesterase inhibitor Mytelase at the age of 42 resulted in a measurable improvement but was discontinued due to significantly increased fatigability, which aggravated a pre-existing depressive disorder.

Tubular aggregates contain STIM1, calsequestrin, RyR1, SERCA and GFPT1 but not DPAGT1

Tubular aggregates are the pathognomonic hallmark of tubular aggregate myopathy (TAM) and can be found as secondary features in a variety of inherited or acquired muscle disorders [28, 34]. To elucidate the composition of the tubular aggregates in our patients, we performed a series of immunolabelling experiments on transverse muscle sections. The tubular aggregates in Patient 1 were positive for different sarcoplasmic reticulum proteins including the Ca^{2+} sensor STIM1, the Ca^{2+} buffer calsequestrin (CASQ1), the Ca^{2+} release channel RyR1 and both ATP-dependent SERCA1 and SERCA2 Ca^{2+} pumps (Figure 3A). We also detected the presence of GFPT1 in the aggregates but not of DPAGT1 (Figure 3B). Of note, the RyR1 signals were more pronounced in the periphery than in the centre of the aggregates, while antibodies targeting STIM1, calsequestrin or SERCA labelled both the centre and the periphery. The same distribution pattern of trapped reticular proteins has previously been observed in patients with tubular aggregate myopathy resulting from pathogenic *ORAI1* variants [35].

ORAI1 is hypoglycosylated in muscle extracts from *DPAGT1* patients

To investigate the functional impact of the identified *DPAGT1* variants and to elucidate the pathomechanisms leading to the formation of

tubular aggregates in the myofibres, we assessed the ratio of glycosylated versus unglycosylated ORAI1 in muscle extracts from Patient 1 (Figure 3C). The muscle biopsy from Patient 2 was entirely used for morphological investigations.

In control muscle samples, both ORAI1α and ORAI1β isoforms were detected as two distinct bands by western blot. Following PNGase F treatment and the cleavage of the N-linked oligosaccharides, both ORAI1 isoforms appeared with a lower molecular weight of 33 and 23 kDa, respectively, corresponding to the predicted protein mass of the amino acid sequence without posttranslational modifications. In contrast, the muscle sample from Patient 1 displayed four bands of moderate signal intensities prior to PNGase F treatment, presumably reflecting the co-existence of glycosylated ORAI1α, unglycosylated ORAI1α, glycosylated ORAI1β and unglycosylated ORAI1β. Cleavage of the N-linked oligosaccharides resulted in two distinct bands corresponding to unglycosylated ORAI1α and ORAI1β. Altogether, these results suggest that ORAI1 is largely glycosylated in control myofibers and only partially glycosylated in muscles from *DPAGT1* patients.

DISCUSSION

Here, we report two patients with early-onset limb-girdle muscle weakness associated with a myasthenic EMG pattern and the presence of ultrastructural NMJ defects and tubular aggregates on muscle biopsies, and we provide clinical, genetic, histological, ultrastructural and functional data. This study expands the mutation spectrum of *DPAGT1*-related LG-CMS, describes the effects of pyridostigmine treatment and delivers insight into the formation of tubular aggregates in the myofibers of affected individuals.

Pathogenic *DPAGT1* variants and genotype/phenotype correlation

Congenital disorders of glycosylation (CDG) encompass a heterogeneous group of systemic diseases caused by abnormal regulation of posttranslational modifications and more specifically of glycosylation. Glycosylation refers to the addition of diverse glycoconjugates to all types of proteins and lipids through glycosyltransferases in the endoplasmic/sarcoplasmic reticulum and the Golgi apparatus [36]. The different CDG subtypes either involve an aberrant oligosaccharide biosynthesis or a defective processing and covalent attachment of the glycans to the nascent glycoprotein, resulting in absent or structurally deviant glycosylation [36]. CDG subtype Ij is caused by pathogenic variants in *DPAGT1*, coding for UDP-N-acetylglucosaminedolichyl-phosphate N-acetylglucosaminephosphotransferase, the enzyme catalysing a primary step of the oligosaccharide synthesis pathway [6]. To date, almost 40 patients from 18 CDGIj families have been described, and in general, they show a severe disease course characterised by marked neonatal hypotonia, joint contractures, intractable epilepsy, cognitive impairment, cataracts and hepatic dysfunction, and most deceased before the age of 5 years [37]. Of note, specific *DPAGT1* variants give rise to LG-CMS, a different and clinically milder disorder. Affected individuals present with infancy or childhood-onset limb-girdle muscle weakness, fluctuating fatigability associated with structural NMJ anomalies and neuromuscular transmission defects, learning disabilities and, in some cases scoliosis, contractures and moderate breathing difficulties [6, 19–23].

Both CDGIj and LG-CMS are autosomal-recessive disorders and both are caused by a similar spectrum of missense and frameshift variants scattered over all coding exons of *DPAGT1*. In agreement, we identified both mutation types in *DPAGT1* exons 2, 3 and 8 in our LG-CMS patients, confirming the absence of an obvious disease-specific mutation hotspot. However, high-impact variants inducing mRNA decay and a strong downregulation of protein expression are overrepresented in CDGIj, and functional investigations in a cell model demonstrated that the CDGIj missense variants impact protein folding or intracellular localization and result in rapid degradation or the absence of the protein at the ER [38]. Altogether, this suggests that the CDGIj-related *DPAGT1* variants largely interrupt the oligosaccharide synthesis pathway, while LG-CMS-related *DPAGT1* variants may impair enzymatic DPAGT1 function and protein glycosylation to a lower degree and cause an overall milder disease phenotype.

The origin of tubular aggregates in LG-CMS

Glycosylation modifies the folding, transport and physical properties of nascent proteins and lipids and thus controls a multitude of biological processes in all cell types [36]. The Ca^{2+} channel ORAI1 carries a single N-glycosylation motif in the extracellular loop between transmembrane segments 2 and 3 [39], and it has been shown that ORAI1 glycosylation is cell type-specific and differently impacts channel function. In the example of immune cells, ORAI1 glycosylation at the Asn223 residue is required for the interaction with negative regulators such as lectins and the absence of proper ORAI1 glycosylation results in channel overactivity without affecting the protein level or the localization of ORAI1 at the plasma membrane [17].

ORAI1 channel gating is also regulated by the Ca^{2+} sensor STIM1, and both are key factors of store-operated Ca^{2+} entry (SOCE), a major mechanism regulating Ca^{2+} balance in all tissues and organs [40, 41]. STIM1 and ORAI1 gain-of-function mutations induce SOCE overactivity and excessive extracellular Ca^{2+} entry and lead to tubular aggregate myopathy (TAM), characterised by structural and functional anomalies of skeletal muscle, bones, platelets, skin and spleen and by the presence of tubular aggregates on muscle biopsies [26, 29, 35, 42–48]. Tubular aggregates were also observed in our patients and six of the previously reported *DPAGT1* families [6, 22]. Investigations on muscle extracts revealed ORAI1 hypoglycosylation in our patients and STIM1 hypoglycosylation in another *DPAGT1* family [22], illustrating that glycosylation defects can occur at different levels of the SOCE pathway and suggesting a causal link with the formation of tubular aggregates in LG-CMS. Indeed, the aggregates in LG-CMS and TAM myofibers were of comparable structure and contained sarcoplasmic

PATHOGENIC *DPAGT1* VARIANTS IN LIMB-GIRDLE CONGENITAL MYASTHENIC SYNDROME (LG-CMS) ASSOCIATED WITH TUBULAR AGGREGATES AND ORAI1 HYPOGLYCOSYLATION

Neuropathology and Applied Neurobiology
JOURNAL OF THE BRITISH NEUROPATHOLOGICAL SOCIETY
WILEY

11 of 13

reticulum proteins as STIM1, the Ca^{2+} buffer calsequestrin, the Ca^{2+} channel RyR1 and the SERCA Ca^{2+} pumps (this study and [35, 49]), indicating that they were formed in a similar way.

Although both GFPT1 and DPAGT1 act in the same glycosylation pathway, only GFPT1 was found in the tubular aggregates in our patients. This is possibly due to the different localization of both proteins within the sarcoplasmic reticulum and demonstrates that not all reticular proteins are sequestered to the aggregates to the same extent. The pathological effect of tubular aggregates on muscle functionality remains to be determined, especially since murine TAM models recapitulate the main features of the disease in the absence of aggregates in muscle fibres [50, 51]. It is, however, possible that the aggregates contribute to the muscle weakness of the LG-CMS patients.

The effect of pyridostigmine treatment

Pyridostigmine is an inhibitor of acetylcholinesterase and thus decelerates the enzymatic breakdown of the neurotransmitter acetylcholine and increases its steady-state level at the NMJ. It is routinely used for the treatment of myasthenia gravis (MG) and other muscle disorders with abnormal neurotransmission [52, 53]. It has also been administrated to single *DPAGT1* patients with a positive outcome [6, 20], but quantitative data or a detailed description of the clinical effect have not been provided. In the present study, we treated our *DPAGT1* patient with pyridostigmine for 6 months, and we observed an amelioration of muscle force and function after an initial treatment period of 21 days and a stabilisation of the condition after 6 months.

However, the overall improvement was mild, and we cannot exclude the possibility that the benefit of pyridostigmine treatment on the 6MWT, arm movement amplitude, pinching force and Moviplate score are at least partially due to a learning effect. Alternatively, the muscle weakness in our patient may only partially result from neurotransmission defects at the postsynaptic membrane and may also reflect a physiological consequence of ORAI1 dysfunction.

It is noteworthy that pyridostigmine treatment also showed a limited effect in other LG-CMS forms. In patients with pathogenic *GFPT1* variants, a measurable response to pyridostigmine treatment was noted, but muscle weakness gradually progressed [54]. *GFPT1* codes for an essential enzyme for the biosynthesis of N-acetylglucosamine, a substrate processed by DPAGT1 in the glycosylation pathway, and patients with pathogenic *GFPT1* variants show tubular aggregates on muscle biopsies [7]. This further supports the idea that pyridostigmine efficiently counteracts the neurotransmission defects associated with abnormal AChR glycosylation, assembly and export to the NMJ [5, 6, 15, 16] but remains ineffective in relieving the muscle phenotype caused by abnormal STIM1 and ORAI1 function.

By contrast, a significant improvement in muscle force was observed in *GFPT1* patients following the administration of salbutamol/albuterol [54–56]. This β2 adrenergic receptor agonist induces airway smooth muscle relaxation and is routinely used to treat asthma. It has also been shown to increase muscle strength in patients with central core disease (CCD) or multi-minicore disease (MmD) associated with pathogenic variants in the ryanodine receptor RyR1 [57, 58], a sarcoplasmic reticulum channel functionally linked to STIM1 and the SOCE pathway. In light of the positive effect in *GFPT1* patients, a combined pyridostigmine and salbutamol/albuterol treatment was proposed for our patients. The efficacy of such a therapy may depend on the disease stage.

AUTHOR CONTRIBUTIONS

ACKNOWLEDGEMENTS

CONFLICT OF INTEREST STATEMENT

None of the authors declare competing interest relating to the present article.

DATA AVAILABILITY STATEMENT

The authors confirm that the data supporting the findings of this study are available within the article.

ETHICS STATEMENT

All patients and legal guardians consent to the publication of the clinical, histological and genetic data. Molecular diagnosis was carried out with written informed consent from the patients or legal guardians. DNA storage and usage were IRB-approved (DC-2012-1693).

ORCID

Johann Böhm https://orcid.org/0000-0001-8019-9504

REFERENCES

1. Engel AG, Shen XM, Selcen D, Sine SM. Congenital myasthenic syndromes: pathogenesis, diagnosis, and treatment. *Lancet Neurol.* 2015;14(4):420-434. doi:10.1016/S1474-4422(14)70201-7

2. Nicole S, Azuma Y, Bauche S, Eymard B, Lochmuller H, Slater C. Congenital myasthenic syndromes or inherited disorders of neuromuscular transmission: recent discoveries and open questions. *J Neuromuscul Dis.* 2017;4(4):269-284. doi:10.3233/JND-170257

3. Evangelista T, Hanna M, Lochmuller H. Congenital myasthenic syndromes with predominant limb girdle weakness. *J Neuromuscular Dis.* 2015;2(Suppl 2):S21-S29. doi:10.3233/JND-150098

4. O'Connor E, Topf A, Zahedi RP, et al. Clinical and research strategies for limb-girdle congenital myasthenic syndromes. *Ann N Y Acad Sci*. 2018;1412(1):102-112. doi:10.1111/nyas.13520

5. Cossins J, Belaya K, Hicks D, et al. Congenital myasthenic syndromes due to mutations in ALG2 and ALG14. *Brain*. 2013; 136(Pt 3):944-956. doi:10.1093/brain/awt010

6. Belaya K, Finlayson S, Slater CR, et al. Mutations in DPAGT1 cause a limb-girdle congenital myasthenic syndrome with tubular aggregates. *Am J Hum Genet*. 2012;91(1):193-201. doi:10.1016/j.ajhg.2012.05.022

7. Guergueltcheva V, Muller JS, Dusl M, et al. Congenital myasthenic syndrome with tubular aggregates caused by GFPT1 mutations. *J Neurol*. 2012;259(5):838-850. doi:10.1007/s00415-011-6262-z

8. Belaya K, Rodriguez Cruz PM, Liu WW, et al. Mutations in GMPPB cause congenital myasthenic syndrome and bridge myasthenic disorders with dystroglycanopathies. *Brain*. 2015;138(Pt 9):2493-2504. doi:10.1093/brain/awv185

9. Beeson D, Higuchi O, Palace J, et al. Dok-7 mutations underlie a neuromuscular junction synaptopathy. *Science*. 2006;313(5795):1975-1978. doi:10.1126/science.1130837

10. Huze C, Bauche S, Richard P, et al. Identification of an agrin mutation that causes congenital myasthenia and affects synapse function. *Am J Hum Genet*. 2009;85(2):155-167. doi:10.1016/j.ajhg.2009.06.015

11. Ohkawara B, Cabrera-Serrano M, Nakata T, et al. LRP4 third beta-propeller domain mutations cause novel congenital myasthenia by compromising agrin-mediated MuSK signaling in a position-specific manner. *Hum Mol Genet*. 2014;23(7):1856-1868. doi:10.1093/hmg/ddt578

12. Chevessier F, Faraut B, Ravel-Chapuis A, et al. MUSK, a new target for mutations causing congenital myasthenic syndrome. *Hum Mol Genet*. 2004;13(24):3229-3240. doi:10.1093/hmg/ddh333

13. Ohno K, Brengman J, Tsujino A, Engel AG. Human endplate acetylcholinesterase deficiency caused by mutations in the collagen-like tail subunit (ColQ) of the asymmetric enzyme. *Proc Natl Acad Sci U S A*. 1998;95(16):9654-9659. doi:10.1073/pnas.95.16.9654

14. Senderek J, Muller JS, Dusl M, et al. Hexosamine biosynthetic pathway mutations cause neuromuscular transmission defect. *Am J Hum Genet*. 2011;88(2):162-172. doi:10.1016/j.ajhg.2011.01.008

15. Gehle VM, Walcott EC, Nishizaki T, Sumikawa K. N-glycosylation at the conserved sites ensures the expression of properly folded functional ACh receptors. *Brain Res Mol Brain Res*. 1997;45(2):219-229. doi:10.1016/S0169-328X(96)00256-2

16. Zoltowska K, Webster R, Finlayson S, et al. Mutations in GFPT1 that underlie limb-girdle congenital myasthenic syndrome result in reduced cell-surface expression of muscle AChR. *Hum Mol Genet*. 2013;22(14):2905-2913. doi:10.1093/hmg/ddt145

17. Dorr K, Kilch T, Kappel S, et al. Cell type-specific glycosylation of Orai1 modulates store-operated Ca2+ entry. *Sci Signal*. 2016;9(418): ra25. doi:10.1126/scisignal.aaa9913

18. Mignen O, Thompson JL, Shuttleworth TJ. STIM1 regulates Ca2+ entry via arachidonate-regulated Ca2+-selective (ARC) channels without store depletion or translocation to the plasma membrane. *J Physiol*. 2007;579(Pt 3):703-715. doi:10.1113/jphysiol.2006.122432

19. Bogdanova-Mihaylova P, Murphy RPJ, Alexander MD, et al. Congenital myasthenic syndrome due to DPAGT1 mutations mimicking congenital myopathy in an Irish family. *Eur J Neurol*. 2018;25(2):e22-e23. doi:10.1111/ene.13532

20. Klein A, Robb S, Rushing E, Liu WW, Belaya K, Beeson D. Congenital myasthenic syndrome caused by mutations in DPAGT. *Neuromuscul Disord*. 2015;25(3):253-256. doi:10.1016/j.nmd.2014.11.013

21. Basiri K, Belaya K, Liu WW, Maxwell S, Sedghi M, Beeson D. Clinical features in a large Iranian family with a limb-girdle congenital myasthenic syndrome due to a mutation in DPAGT1. *Neuromuscul Disord*. 2013;23(6):469-472. doi:10.1016/j.nmd.2013.03.003

22. Selcen D, Shen XM, Brengman J, et al. DPAGT1 myasthenia and myopathy: genetic, phenotypic, and expression studies. *Neurology*. 2014;82(20):1822-1830. doi:10.1212/WNL.0000000000000435

23. Finlayson S, Palace J, Belaya K, et al. Clinical features of congenital myasthenic syndrome due to mutations in DPAGT1. *J Neurol Neurosurg Psychiatry*. 2013;84(10):1119-1125. doi:10.1136/jnnp-2012-304716

24. Barone V, del Re V, Gamberucci A, et al. Identification and characterization of three novel mutations in the CASQ1 gene in four patients with tubular aggregate myopathy. *Hum Mutat*. 2017;38(12):1761-1773. doi:10.1002/humu.23338

25. Bohm J, Lornage X, Chevessier F, et al. CASQ1 mutations impair calsequestrin polymerization and cause tubular aggregate myopathy. *Acta Neuropathol*. 2018;135(1):149-151. doi:10.1007/s00401-017-1775-x

26. Bohm J, Chevessier F, Maues De Paula A, et al. Constitutive activation of the calcium sensor STIM1 causes tubular-aggregate myopathy. *Am J Hum Genet*. 2013;92(2):271-278. doi:10.1016/j.ajhg.2012.12.007

27. Nesin V, Wiley G, Kousi M, et al. Activating mutations in STIM1 and ORAI1 cause overlapping syndromes of tubular myopathy and congenital miosis. *Proc Natl Acad Sci U S A*. 2014;111(11):4197-4202. doi:10.1073/pnas.1312520111

28. Chevessier F, Bauche-Godard S, Leroy JP, et al. The origin of tubular aggregates in human myopathies. *J Pathol*. 2005;207(3):313-323. doi:10.1002/path.1832

29. Morin G, Biancalana V, Echaniz-Laguna A, et al. Tubular aggregate myopathy and Stormorken syndrome: mutation spectrum and genotype/phenotype correlation. *Hum Mutat*. 2020;41(1):17-37. doi:10.1002/humu.23899

30. Servais L, Deconinck N, Moraux A, et al. Innovative methods to assess upper limb strength and function in non-ambulant Duchenne patients. *Neuromuscul Disord*. 2013;23(2):139-148. doi:10.1016/j.nmd.2012.10.022

31. Hogrel JY, Decostre V, Ledoux I, et al. Normalized grip strength is a sensitive outcome measure through all stages of Duchenne muscular dystrophy. *J Neurol*. 2020;267(7):2022-2028. doi:10.1007/s00415-020-09800-9

32. Thomas KC, Zheng XF, Garces Suarez F, et al. Evidence based selection of commonly used RT-qPCR reference genes for the analysis of mouse skeletal muscle. *PLoS ONE*. 2014;9(2):e88653. doi:10.1371/journal.pone.0088653

33. McDonald CM, Henricson EK, Han JJ, et al. The 6-minute walk test as a new outcome measure in Duchenne muscular dystrophy. *Muscle Nerve*. 2010;41(4):500-510. doi:10.1002/mus.21544

34. Goebel HH. When tubules aggregate. *Neuromuscul Disord*. 2012; 22(3):208-210. doi:10.1016/j.nmd.2011.12.006

35. Bohm J, Bulla M, Urquhart JE, et al. ORAI1 mutations with distinct channel gating defects in tubular aggregate myopathy. *Hum Mutat*. 2017;38(4):426-438. doi:10.1002/humu.23172

36. Reily C, Stewart TJ, Renfrow MB, Novak J. Glycosylation in health and disease. *Nat Rev Nephrol*. 2019;15(6):346-366. doi:10.1038/s41581-019-0129-4

37. Ng BG, Underhill HR, Palm L, et al. DPAGT1 deficiency with encephalopathy (DPAGT1-CDG): clinical and genetic description of 11 new patients. *JIMD Rep*. 2019;44:85-92. doi:10.1007/8904_2018_128

38. Yuste-Checa P, Vega AI, Martin-Higueras C, et al. DPAGT1-CDG: functional analysis of disease-causing pathogenic mutations and role of endoplasmic reticulum stress. *PLoS ONE*. 2017;12(6):e0179456. doi:10.1371/journal.pone.0179456

39. Gwack Y, Srikanth S, Feske S, et al. Biochemical and functional characterization of Orai proteins. *J Biol Chem*. 2007;282(22):16232-16243. doi:10.1074/jbc.M609630200

PATHOGENIC *DPAGT1* VARIANTS IN LIMB-GIRDLE CONGENITAL MYASTHENIC SYNDROME (LG-CMS) ASSOCIATED WITH TUBULAR AGGREGATES AND ORAI1 HYPOGLYCOSYLATION

Neuropathology and Applied Neurobiology
JOURNAL OF THE BRITISH NEUROPATHOLOGICAL SOCIETY

WILEY | **13 of 13**

40. Feske S, Gwack Y, Prakriya M, et al. A mutation in Orai1 causes immune deficiency by abrogating CRAC channel function. *Nature*. 2006;441(7090):179-185. doi:10.1038/nature04702

41. Zhang SL, Yu Y, Roos J, et al. STIM1 is a Ca2+ sensor that activates CRAC channels and migrates from the Ca2+ store to the plasma membrane. *Nature*. 2005;437(7060):902-905. doi:10.1038/nature04147

42. Bohm J, Laporte J. Gain-of-function mutations in STIM1 and ORAI1 causing tubular aggregate myopathy and Stormorken syndrome. *Cell Calcium*. Sep 3 2018;76:1-9. doi:10.1016/j.ceca.2018.07.008

43. Endo Y, Noguchi S, Hara Y, et al. Dominant mutations in ORAI1 cause tubular aggregate myopathy with hypocalcemia via constitutive activation of store-operated Ca(2)(+) channels. *Hum Mol Genet*. 2015;24(3):637-648. doi:10.1093/hmg/ddu477

44. Misceo D, Holmgren A, Louch WE, et al. A dominant STIM1 mutation causes Stormorken syndrome. *Hum Mutat*. 2014;35(5):556-564. doi:10.1002/humu.22544

45. Morin G, Bruechle NO, Singh AR, et al. Gain-of-function mutation in STIM1 (P.R304W) is associated with Stormorken syndrome. *Hum Mutat*. 2014;35(10):1221-1232. doi:10.1002/humu.22621

46. Netzer C, Bohlander SK, Hinzke M, Chen Y, Kohlhase J. Defining the heterochromatin localization and repression domains of SALL1. *Biochim Biophys Acta*. 2006;1762(3):386-391. doi:10.1016/j.bbadis.2005.12.005 S0925-4439(05)00183-3 [pii]

47. Lacruz RS, Feske S. Diseases caused by mutations in ORAI1 and STIM1. *Ann N Y Acad Sci*. 2015;1356(1):45-79. doi:10.1111/nyas.12938

48. Silva-Rojas R, Laporte J, Bohm J. STIM1/ORAI1 loss-of-function and gain-of-function mutations inversely impact on SOCE and calcium homeostasis and cause multi-systemic mirror diseases. *Front Physiol*. 2020;11:604941. doi:10.3389/fphys.2020.604941

49. Bohm J, Chevessier F, Koch C, et al. Clinical, histological and genetic characterisation of patients with tubular aggregate myopathy caused by mutations in STIM1. *J Med Genet*. 2014;51(12):824-833. doi:10.1136/jmedgenet-2014-102623

50. Silva-Rojas R, Charles AL, Djeddi S, Geny B, Laporte J, Bohm J. Pathophysiological effects of overactive STIM1 on murine muscle function and structure. *Cell*. 2021;10(7):1730. doi:10.3390/cells10071730

51. Silva-Rojas R, Treves S, Jacobs H, et al. STIM1 over-activation generates a multi-systemic phenotype affecting the skeletal muscle, spleen, eye, skin, bones and immune system in mice. *Hum Mol Genet*. 2019;28(10):1579-1593. doi:10.1093/hmg/ddy446

52. Maggi L, Mantegazza R. Treatment of myasthenia gravis: focus on pyridostigmine. *Clin Drug Investig*. 2011;31(10):691-701. doi:10.2165/11593300-000000000-00000

53. Saito M, Ogasawara M, Inaba Y, et al. Successful treatment of congenital myasthenic syndrome caused by a novel compound heterozygous variant in RAPSN. *Brain Dev*. 2022;44(1):50-55. doi:10.1016/j.braindev.2021.09.001

54. Jiang K, Zheng Y, Lin J, et al. Diverse myopathological features in the congenital myasthenia syndrome with GFPT1 mutation. *Brain Behav*. 2022;12(2):e2469. doi:10.1002/brb3.2469

55. Ma Y, Xiong T, Lei G, et al. Novel compound heterozygous variants in the GFPT1 gene leading to rare limb-girdle congenital myasthenic syndrome with rimmed vacuoles. *Neurol Sci*. 2021;42(8):3485-3490. doi:10.1007/s10072-020-05021-0

56. Selcen D, Shen XM, Milone M, et al. GFPT1-myasthenia: clinical, structural, and electrophysiologic heterogeneity. *Neurology*. 2013;81(4):370-378. doi:10.1212/WNL.0b013e31829c5e9c

57. Messina S, Hartley L, Main M, et al. Pilot trial of salbutamol in central core and multi-minicore diseases. *Neuropediatrics*. 2004;35(5):262-266. doi:10.1055/s-2004-821173

58. Schreuder LT, Nijhuis-van der Sanden MW, de Hair A, et al. Successful use of albuterol in a patient with central core disease and mitochondrial dysfunction. *J Inherit Metab Dis*. 2010;33(Suppl 3):S205-S209. doi:10.1007/s10545-010-9085-7